Journal Article

Characterisation and solution properties of a galactomannan from *Bauhinia monandra* seeds

Louis M. Nwokocha; Chandra Senan; Peter A. Williams, Madhav P. Yadav

Recommended citation:

Nwokocha, Louis M., Senan, C, Williams, P.A., Yadav, M.P. (2017), 'Characterisation and solution properties of a galactomannan from Bauhinia monandra seeds', International Journal of Biological Macromolecules, vol 101, pp.904–909. doi: /10.1016/j.ijbiomac.2017.03.105.

Characterisation and solution properties of a galactomannan from *Bauhinia monandra* seeds

Louis M. Nwokocha[1]; Chandra Senan[2]; Peter A. Williams[2,*], Madhav P. Yadav[3]
[1]Department of Chemistry, University of Ibadan, Ibadan, Nigeria

[2]Center for Water Soluble Polymers, Glyndwr University, Wrexham,
LL 11 2AW, North Wales, UK
[3]United States Department of Agriculture-ARS, Eastern Regional Research Center, 600 East Mermaid Lane, Wyndmoor, Philadelphia 19038, PA, USA.

*Corresponding author. Tel.: +44 1978293 083.

E-mail address: p.a.williams@glyndwr.ac.uk (P.A. Williams).

Abstract

This study reports on the chemical and physicochemical properties of the polysaccharide isolated from *Bauhinia monandra* seeds. The seeds were found to contain 17.8% polysaccharide which consisted predominantly of galactose and mannose. The Man/Gal ratio was found to be approximately 4:1and the average molar mass was 2.54 x 10^5 g/mol. The extracted material was also found to contain a small amount of protein (5.35%). The galactomannan produced highly viscous solution, the viscosity – shear rate profile was best described by the Williamson model. The mechanical spectrum of a 0.5 wt% solution showed that G″ was greater than G′ over the frequency range employed while at higher concentrations G′ became greater than G″ above a critical frequency. The solutions obeyed the Cox-Merz rule at low concentrations but there was some deviation at higher concentrations. Viscosity measurements were undertaken over a range of temperatures and the activation energy of viscous flow was found to be 20.75 kJ/mol. The rheological properties of solutions of *B. monandra* galactomannan indicate that it has comparable characteristics to other commercially important galactomannans such as guar gum and locust bean gum and hence has potential as a thickener in the formulation of food and other related products.

Key words: *Bauhinia monandra*; galactomannan; solution characteristics

1. Introduction

Bauhinia monandra Kurz belongs to the family *Caesalpiniaceae* and about 250 species of the *Bauhinia* genus are known [1]. *B. monandra* is an ornamental plant usually grown to beautify the environment. The tree bears flat pods containing about 10-20 seeds per pod. The seed contains a polysaccharide which consists of a main chain of D-mannopyranose units and the D-galactopyranose unit is present as the side chain [1]. Seed galactomannans find application as rheology modifiers in a variety of industrial processes. The M/G ratio influences the properties of the galactomannan polysaccharides in water including solubility and gel formation [2]. In the food industry they are used to alter product texture and viscosity and control the distribution of solids in aqueous sols in such a way that a range of texture and mouth feel is produced [3]. Aqueous polysaccharide solutions can be successfully used as model fluids in order to simulate the complex rheological behaviour of materials employed in various technological processes [4]. In the petroleum industry, galactomannans are used as drilling mud modifiers to suspend clay and increase oil recovery [3]. The oil industry employs biopolymers due to their high swelling at low polymer concentrations**;** high efficiency as suspending agents**;** high shear thinning behaviour and exceptional compatibility with high concentrations of various salts and temperatures. To date there has not been a systematic study of the physicochemical characteristics and rheological properties of the polysaccharide from *B. monandra* which has considerable commercial potential. The aim of this work therefore is to isolate the water soluble galactomannan component of *B. monandra* and determine the physicochemical and rheological properties and compare them with those of guar and locust bean gums, two widely applied commercial thickeners. The data obtained would be useful in assessing the

potential of *B. monandra* as an alternative to guar gum and LBG in industrial application.

2. Experimental

2.1 Isolation of galactomannan from seed

Dried pods of *B. monandra* were collected from trees growing in the compounds of the University of Ibadan and The Polytechnic, Ibadan. The pods were dehulled and the seeds collected. The galactomannan extraction procedure was similar to the method described in [5].

The seeds were pulverized with a hammer mill, packed into a Soxhlet extractor and defatted with hexane. A known weight of the defatted flour (10%, w/v) was swollen in water at 60^{o}C overnight and blended using a Warring blender. The slurry was poured into centrifuge bottles and centrifuged at 2500 rpm for 2 h. The supernatant was decanted and residue reconstituted with water and centrifuged again. The supernatants were pooled and the galactomannan precipitated with excess isopropanol. This was reconstituted in a small amount of water and transferred to round bottomed flasks (to prevent the sample drying as lumps), frozen and the galactomannan recovered as powder by drying in a freeze dryer.

2.2 **Determination of protein content of *B. monandra* galactomannan**

The protein (N X 6.25) content was determined by AACC Approved Method 46-30.01 using Flash 2000 protein Analyzer from CE Elantech, Inc. [6]. In brief, the sample was weighed in a tin capsule and introduced into the combustion reactor via autosampler together with a proper amount of pure oxygen. After combustion, the produced gases were carried by a constant helium flow to a second reactor filled with copper reducer, then swept through CO_2 and H_2O traps, a GC column and finally detected by a thermal conductivity detector. A complete N/Protein report was automatically generated by the Eager Xperience dedicated software. The analysis conditions were as follows:

Combustion temperature 900°C, reduction temperature 680°C, oven temperature 50 °C, Helium flow rate 140 ml/min, Oxygen flow rate 100 ml/min and total run time about 5 minutes.

2.3 Determination of sugar composition

The sugar composition was determined by HPAEC-PAD using methanolysis combined with TFA hydrolysis [*7*] with some modification. In brief, the gum sample was first dissolved in de-ionized water (1 mg/ml). An aliquot of 100 nmoles myo-inositol (internal standard) was added to the gum solution and dried in a Teflon-lined screw cap glass vial by blowing with filtered nitrogen followed by drying in a vacuum oven at 50^{o}C overnight. These samples were methanolyzed with 1.5 M methanolic HCl in the presence of 20% (v/v) methyl acetate for 16 h, cooled to room temperature and dried by blowing with filtered N_2 after adding five drops of t-butanol. The methanolyzed samples were hydrolyzed with 0.5 ml 2M TFA at 121^{o}C for 1 h, evaporated by blowing with filtered N_2 at 50^{o}C and the residue was washed by sequential addition and evaporation of three aliquots (0.5 ml) of methanol. In five separate glass vials were placed 100, 200, 300, 500 and 1000 nmoles of a mixture of standard sugars containing fucose, arabinose, rhamnose, galactose, glucose, xylose, glucuronic acid and galacturonic acid. Then, 100 nmoles of myo- inositol (internal standard) was added to each vial, evaporated and dried as above. These standard samples were also methanolyzed and hydrolyzed as described above and used for quantification. Hydrolyzates were analyzed for neutral and acidic sugars by HPAEC-PAD using a Dionex DX-500 system that included a CarboPac PA20 column and guard column, a GP 50 gradient pump, an ED40 electrochemical detector utilizing the quadruple potential waveform (gold working electrode and pH reference electrode), an AS3500 autosampler with a thermal compartment (30EC column-heater), and a PC10 pneumatic

controller post column addition system. The mobile phase consisted of isocratic 12 mM NaOH eluant for 10 min followed by 100 mM NaOH and 6 mM CH_3COONa for 3 min, 100 mM NaOH and 12 mM CH_3COONa for 17 min at a flow rate of 0.5 ml/min. at ambient temperature. The column wash with 1 M CH_3COONa for 0.10 min and 100 mM NaOH for 10 min followed by 30-min equilibration with 12 mM NaOH at a flow rate of 0.5 ml/min at ambient temperature was required to yield highly reproducible retention times for the monosaccharides. The total run time was ca. 70 min. In order to minimize baseline distortion due to change in pH of the eluant during monosaccharides detection by PAD, 730 mM NaOH was added to the post column effluent via a mixing tee.

2.4 Molecular mass determination

The eluent, (0.1M $NaNO_3$ with sodium azide biocide in deionized water) was initially passed through a 0.22 µm type GSWP mixed cellulose ester Millipore membrane filter. A 5 mg/ml solution of the *B. monandra* was prepared in the eluent by vigorous shaking overnight in a Stuart Scientific orbital incubator and with a Stuart flask shaker the next day. It was subsequently heated (85^oC) for 4 min in a water bath, followed by sonication at full power using a Soniprep 150 MSE sonicator. As the sample was deemed to be too viscous, it was diluted with eluent to give a 2 mg/ml solution which was then used for GPC analysis.

The sample solution was filtered through a 0.45 µm nylon syringe filter to fill the 200 uL loop of the Rheodyne valve system linked to the rest of the GPC instrumentation, prior to injection into a Suprema column (3000Å, 8 x 300 mm) packed with 10 µm beads comprising a polyhydroxymethacrylate copolymer network. The eluent was pumped (Waters: 515 HPLC Pump, Milford, MA 01757, USA) through an in-line eluent degasser (CSI 6150, Cambridge Scientific Instruments, England) at a flow rate of 0.5 ml/min. The total injected mass was 4.11 x 10^{-4} g. The detector array comprised

a Dawn DSP laser photometer (MALLS detector) and Optilab DSP interferometric refractometer viz. RI detector).The GPC/MALLS chromatogram was analyzed using ASTRA software (Astra for Windows 4.90.08 QELLS 2 . xx) using the Berry model with first order polynomial and a dn/dc value of 0.140 ml/g

2.5 Rheological studies

Galactomannan solutions (0.5 - 2.0wt%) were prepared by dispersing the powder in the required volume of distilled water on a roller mixer overnight at room temperature after which time the sample was fully dissolved. Rheological measurements carried out according to the procedure in [5]. Studies were done at 25^{o}C using a controlled stress rheometer (T.A. Instruments, USA) with cone and plate geometry (40mm 2° steel cone, ser no 982525; gap 53 micro m). The sample was placed on the Peltier plate with a spoon spatula, the cone was lowered and gap set, and the excess sample trimmed off. In all the studies, low viscosity oil was applied around the edge of the cone to act as a solvent trap.

2.5.1. Steady shear viscosity: Under steady shear, the galactomannan solutions were subjected to a steady stepped flow procedure at a shear rate of 0.01 – 1000 s^{-1}. The viscosity data obtained were analyzed using the Williamson model (Eq. 1) in the T.A. data analysis software

$$\frac{\eta}{\eta_o} = \frac{1}{(1+(\tau * \dot{\gamma})^N)} \qquad \text{(Eq. 1)}$$

where η, η_o are shear and zero shear viscosities, respectively; $\dot{\gamma}$, τ and N are shear rate, Williamson relaxation time and Williamson rate index, respectively.

2.5.2. Small deformation oscillation experiments: Under oscillatory shear, the stress sweep was carried out at oscillation stress of 0.01- 500 Pa at a fixed frequency of 1Hz, with the aim to locate the linear viscoelastic region. Then a frequency sweep was conducted using an oscillation stress value in the linear viscoelastic region to obtain the frequency sweep data.

2.4.3 Effect of temperature: The effect of temperature on the apparent viscosity was investigated on a 2% galactomannan solution by carrying out a stepped flow procedure at different temperatures (15^{o}C to 50^{o}C) over the shear rate range 0.01 – 1000 s^{-1}. The flow curves were fitted to the Williamson model and the zero shear viscosities (η_o) at different temperatures determined. The η_o was plotted against the inverse of the absolute temperature (T). The activation energy for viscous flow was estimated using the modified Arrhenius equation (Eq. 2)

$$\eta_o = \eta_{o,T_\infty} \exp\left(\frac{E_a}{RT}\right) \qquad \text{(Eq. 2)}$$

Where η_o= zero shear viscosity (Pa s) at temperature (T)**;** η_{o,T_∞}= zero shear viscosity (Pa s) at infinite temperature (T_∞)**;** Ea = activation energy (J/mol)**;** R = universal gas constant (8.314 J/mol/K**;** T= temperature (K).Since η_{o,T_∞} represents the zero shear viscosity at infinite temperature, the equation can be written in the natural logarithmic form by choosing a reference temperature, in this case 298^{o}K (Eq. 3).

$$\ln \eta_o = \ln \eta_{o,298} + \frac{E_a}{R}\left(\frac{1}{T} - \frac{1}{298}\right) \qquad \text{(Eq. 3)}$$

3. Results and Discussion

3.1 Yield, protein content and monosaccharide composition

The yield of galactomannan from the *B. monandra* seeds (Table 1) was 17.8% and is close to 19% reported for *B. malabania* seed by [8].The gum yield is less than 20. 4 % reported for *Peltophorum pterocarpum* seed [5], 26% reported for *Cassia javanica* seeds [9] and 40 – 61.7% reported for LBG [10, 11]. The galactomannan from *B. monandra* had a protein content of 5.35% which is less than 11.69% protein reported for *Mucuna flagellipes* polysaccharide [12] and 6.9 – 10.3% reported for LBG [10].

B. monandra galactomannan (Table 1) contained mannose (77.28%), galactose (19.32%), and small amounts of glucose (2.44%), arabinose (0.52%} and glucuronic acid (0.44%). These results indicate that *B. monandra* is a glactomannan with Man/Gal

ratio of 4:1. The Mal/Gal ratio is higher than 3.2:1 reported for *B. malabania* galactomannan [13], 2:1 reported for guar [11], slightly less than 4.4:1 reported for *Peltophorum pterocarpum* [5] but comparable to 4:1 reported for LBG [14]. This suggests *B. monandra* glactomannan would have similar solution properties to LBG.

3.2 Molecular characteristics of *B. monandra* galactomannan

The GPC-MALLS of *B. monandra* galactomannan (Figure 1) shows presence of two components, with the major component eluting at 8.0 ml (peak 1) and a minor component eluting at 12 ml (peak 2). The molar mass values were obtained by fitting the data to a Berry plot and are presented in Table 1. The whole polysaccharide had an average molar mass (M_w) of 2.54 x 10^5g/mol, the polydispersity index (M_w/M_n) was 1.37 while the radius of gyration (R_g) was 40.7 nm. The analysis of the two eluted components separately showed that the major component (Peak 1) had M_w = 2.73x 10^5 g/mol, M_w/M_n = 1.17, R_g = 41.4 nm) while the minor component (Peak 2) had M_w = 1.25 x 10^5 g/mol, M_w/M_n = 1.00, R_g = 34.7 nm. We have not presently found any literature on the molar mass of *B .monandra* galactomannan for comparison. Since *B. monandra* galactomannan has similar M/G ratio as found in LBG it would be proper to compare their M_w. Haddarah et al. [11] and Gaisford et al. [10] have reported M_w in the range of 3.0 - 13.8 x 10^5 g/mol for LBG which is close to the value obtained for *B. monandra*.

3.3 Flow properties of *B. monandra* galactomannan under steady shear

The result of steady shear studies carried out on solutions of 0.5 – 2.0wt%, *B. monandra* galactomannan are presented in Figure 2a. The flow parameters obtained by fitting the flow curves to the Williamson model are presented in Table 2a.

The galactomannan solutions exhibited two shear flow regimes. A low shear Newtonian regime in which the apparent viscosity remained constant as shear rate increased and a

shear thinning regime in which the apparent viscosity decreased with increasing shear rate.

The transition from a Newtonian to a shear thinning regime occurred at a critical shear rate ($\dot{\gamma}_{Cr}$). The $\dot{\gamma}_{Cr}$ shifted to lower shear rates as polymer concentration increased (Table 2a). This shear rate marked the onset of shear thinning. The critical shear rate is related to the relaxation time, τ through $\tau = 1/\dot{\gamma}_{Cr}$. The τ is the time taken by the polymer macromolecules to relax from all imposed stress brought about by shearing action. The value of τ increased with increase in polymer concentration. This is because at higher concentrations, the polymer coils are enmeshed and interpenetrate one another and when subjected to shear, these polymer coils become strained. After the imposed stress is removed, the time for stress relaxation is directly proportional to the number of entanglements. At a concentration of 0.5%, the η_o was 0.25 Pa s and increased to 244 Pa s at 2.0%. In comparison the apparent viscosity of *B. monandra* at 1% dispersion (7.179 Pa s) was in the range of values reported for guar (6.0 – 7.5 Pa s) but higher than that reported for LBG (3.0 -3.5 Pas) [15, 16]

The high zero shear apparent viscosity of *B. monandra* is a positive application property of the galactomannan as both suspending agent and stabilizer. The rate index lay between 0.5117- 0.7383 and increased with rise in galactomannan concentration. This indicates the degree of dependence of viscosity on shear rate in the shear thinning region for the *B. monandra* galactomannan. The strong shear thinning characteristics is a positive attribute for this galactomannan because it makes operations such as mixing, pumping, packaging or bottling easier [17].

The dependence of viscosity on concentration could be reduced to a master curve by a plot of the reduced variables η/η_o versus $\tau\dot{\gamma}$. The Figure 2b indicates that $\eta/\eta_o \sim 1$ as $\tau\dot{\gamma} \sim 0$.

3.4 Viscoelastic properties of *Bauhinia monandra* galactomannan

The linear viscoelastic region fell in the range of oscillation stress 0.1 – 1.0 Pa (Figure S1), therefore an oscillation stress of 0.5 Pa within this range was applied to generate the frequency sweep data.

Figure 3 shows the variation of G′ and G″ with angular frequency, ω, at different polymer concentrations. The galactomannan exhibited viscous properties at polymer concentrations of 0.5% and below**,** with G″> G′ at all concentrations**.** However, both G′ and G″ showed dependence on ω with the separation between both moduli getting narrower as ω increased although no crossover occurred. However, polymer concentrations between 0.75% to 2.0% exhibited viscoelastic properties with both moduli crossing over (G′ = G″) at a critical angular frequency (ω_{crit}) below which the polymer solution exhibited a predominantly viscous response viz. G″ > G′. In contrast, above ω_{crit}, the solution exhibited a predominantly elastic response (G′ > G″). The value of G at the crossover point increased as concentration increased while the ω_{crit} decreased (Table 2b).The time for microstructural coupling (τ′) [given as $\tau' = 1/\omega_{crit}$] increased with increase in polymer concentration. The complex modulus, G* is related to complex viscosity η* by $|\eta^*| = |G^*|/\omega$ and $|G^*| = (|G'|^2 + |G''|^2)^{1/2}$. The relationship between steady shear ($\eta(\dot{\gamma})$) and its oscillatory analogue ($|\eta^*(\omega)|$) was tested by superimposing the two sets of data for $\dot{\gamma} = \omega$. This relationship is referred to as the Cox-Merz superimposition. When this rule is valid, the rheological properties can be determined by either oscillatory or steady-state shear experiments, both of which are useful due to the limitations in each kind of experiment [18]. In addition, the Cox-Merz rule provides information about the microstructure of the materials from their degree of conformity with the rule [19].

As can be seen from Figure 4, the Cox-Merz superimposition was closely obeyed at 0.5 wt% but deviations became more pronounced at higher concentrations and higher shear rates. This divergence has been attributed to enthalpic association between the macromolecules. Such associations include various types of specific and non-specific interactions, some of which could only survive oscillatory (reversible) shear but not steady (destructive or irreversible) shear. Where association is purely topological, complete superimposition is obtained [20].

3.5 Effect of temperature on the flow properties of *B. monandra* galactomannan

The most widespread approach to modelling the effect of temperature on rheological properties is to consider its effect on apparent viscosity. Figure 5a shows that the apparent viscosity of *B. monandra* galactomannan solution decreased with rising temperature.

The apparent zero shear viscosity at 15^{o}C was 633.6 Pa s while at 50^{o}C it was 209 Pa s. Similar observations have been reported for other polysaccharides [20, 21]. Changes in viscosity with temperature can be used to manipulate the properties of polysaccharide-thickened media. For instance, the addition of thermal energy to a system will increase the vibrational energy of the molecules and thereby weaken the inter- and intra-molecular associations resulting in ready flow. By removing thermal energy, the inter- and intra-molecular associations are increased**,** inducing gel formation. This has been attributed to extended inter-particle associations at low temperatures [21].The activation energy(E_a) for viscous flow of 2wt% *B. monandra* galactomannan was estimated from the Arrhenius plot of the zero shear viscosity as a function of the inverse of absolute temperature (Figure 5b).

The E_a was calculated to be 20.75 kJ/mol, this being the energy barrier that must be overcome before elementary flow processes can occur [22].This value signifies the

minimum energy required to initiate flow in a 2 wt% solution of *B. monandra* seed galactomannan. In addition to temperature, E_a has also been reported to be affected by polymer concentration, the nature of intra- and inter-chain interactions and the molecular mass of the polysaccharide [20, 23].

4. Conclusions

We have isolated the water soluble galactomannan constituent of *B. monandra* seed and characterised it. The galactomannan had Man/Gal ratio, molar mass and rheological properties similar to LBG and can be a good substitute in applications in which LBG is employed. Thus *B. monandra* has the potential to be used as thickener in food and related products.

5. References

[1]. B.K. Srivastava; G. Chandra; D. Saxena & A. Kumar (2010). Methylation study of polysaccharides from seeds of *Bauhinia purpurea*. Oriental Journal of Chemistry 26(2), 673-676.

[2]. V. Mathur & N. K. Mathur (2005). Fenugreek and other lesser known legume galactomannan-polysaccharides: scope for developments. Journal of Scientific and Industrial Research, 64, 475-481.

[3]. N. K. Mathur (2011). Applications of galactomannan hydrocolloids in food and non-food industries. Industrial Galactomannan Polysaccharides. CRC Press.

[4]. U. Florjancic; A. Zupancic & M. Zumer (2002). Rheological characterization of aqueous polysaccharide mixtures undergoing shear. *Chem. Biochem. Eng. Q.* 16 (3) 105–118.

[5]. L. M. Nwokocha & P. A. Williams (2014a). Isolation and characterization of a novel

polysaccharide from seeds of *Peltophorum pterocarpum*. *Hydrocolloids 41, 319-324.*

[6]. American Association of Cereal Chemists (1999). Approved Method of Analysis, 11th Ed., Crude Protein Combustion Method 46-30.01, AACC International, St. Paul, MN, USA

[7]. M.P. *Yadav;* D.B. *Johnston*; A.T. *Hotchkiss* & K.B. *Hicks (2007).* Corn fiber gum: A potential gum arabic replacer for beverage flavor emulsification**.** *Food Hydrocolloids 21*(7), *1022 – 1030.*

[8]. V. Dubey & M. Lohan (2013). Glycosyl composition and linkages of polysaccharide from *Bauhinia malabania*. Asian Journal of Science and Research 3(3), 91-94.

[9]. E. G. Azero; L. L. Lopes; & C. T. Andrade (1997). Extraction and solution properties

of the galactomannan from the seeds of Cassia javanica L. Polymers Bulletin, 39(5), 621-625.

[10]. S.E. Gaisford; S. E. Harding; J. R. Mitchell & T. D. Bradley. (1986). A comparison between the hot and cold water soluble fractions of two locust bean gum samples. Carbohydrate Polymers 6, 423-442.

[11]. A. Haddarah, A. Bassal, A. Ismail, C. Gaiani, I. Ioannou, C. Charbonnel, T. Hamieh, & M. Ghoul. (2014). The structural characteristics and rheological properties of Lebanese locust bean gum. Journal of Food Engineering 120, 204–214.

[12]. L. M. Nwokocha & P. A. Williams (2009). Isolation and rheological characterization of *Mucuna flagellipes* seed gum. Food Hydrocolloids 23, 1394–1397.

[13]. M.S. Buckeridge; S.M.C. Dietrich & D.U. de Lima (2000). Galactomannans as reserve carbohydrate in legume seeds. In: Carbohydrate Reserve in Plants-Synthesis and Regulation. A.K. Gupta and N. Kaur (Eds) p283-316. Elsevier Science B.V.

[14]. D.R. Picout; S.B. Ross-Murphy; K. Jumel & S.E. Harding (2002). Pressure Cell Assisted Solution Characterization of Polysaccharides. 2. Locust Bean Gum and Tara Gum. Biomacromolecules 3, 761-767

[15]. D. Saha & S. Bhattacharya 2010. Hydrocolloids as thickening and gelling agents in food: a critical review. Journal of Food Science and Technology 47(6): 587–597.

[16]. R.J. Alexander. (1999) Hydrocolloid gums. Part I: Natural products. Cereal Foods World. 44, 684–687.

[17]. F. Rincon; J. Munoz; P. Ramírez; H. Galan & M. C. Alfaro (2014). Physicochemical

and rheological characterization of *Prosopis juliflora* seed gum aqueous dispersions.

Food Hydrocolloids, 35, 348-357.

[18]. S. Gunasekaran & M.M. Ak (2000). Dynamic oscillatory shear testing of foods-Selected applications. Trends in Food Science and Technology 11, 115–127.

[19]. X. Liu; Y. Luo; C. Zha; S. Zhou; L. Liu & L. Zhao (2015). Rheological properties of polysaccharides from longan (*Dimocarpus longan* Lour.) fruit. International Journal of Polymer Science,Volume 2015, Article ID 168064, 1-5. http://dx.doi.org/10.1155/2015/168064

[20]. L. M. Nwokocha & P. A**.** Williams (2014b).Solution properties of *Brachystegia eurycoma* seed polysaccharide. In: P.A. Williams and G.O. Phillips

(Editors).Gums and Stabilizers for the Food Industry 17: The Changing Face of Food Manufacture: The Role of Hydrocolloids. pp123-138. Royal Society of Chemistry, Cambridge, United Kingdom.

[21]. S.W. Cui (2001). Yellow mustard. In: Polysaccharide Gums from Agricultural Products: Processing, Structure and Functionality. pp 39-40. Technomic Publishing Company Inc., Lancaster, USA.

[22]. M.A. Rao (2014). Rheology of fluid, semisolid and solid foods. Principles and Applications. Third Edition. G. V. Barbosa-Canovas (Series Editor) Food Engineering Series, p52. Springer Science, NY, USA.

[23]. R.C.M. de Paula & J.F. Rodrigues (1995). Composition and rheological properties of cashew tree gum, the exudate polysaccharide from *Anacardium occidentale* L. Carbohydrate Polymers 26 (3), 177–181.

Table 1. Some properties of *B. monandra* seed galactomannan

Yield (%)	17.8		
Protein (%)	5.35±0.06		
Monosaccharide composition (%)[a]			
Ara	0.52±0.05		
Gal	19.32±0.26		
Glc	2.44±0.04		
Man	77.28±0.26		
GlcA	0.44±0.15		
Man/Gal	4/1		
Molecular characteristics[b]	**Total elution**	**Peak 1**	**Peak 2**
Molar mass, M_w (g/mol)	2. 54±0.00 x 10^5	2.73±0. 00 x 10^5	1.25±0.14 x 10^5
Radius of gyration, R_g (nm)	40.7±0.0	41.4±0.8	34.7±0.00
Polydispersity, M_w/M_n	1.28±0.00	1.17±0.00	1.00±0.00

[a] Results are mean±std of triplicate determinations. Note: Ara, Arabinose; Gal, Galactose; Glc, Glucose; Man, Mannose; GlcA, Glucuronic acid

[b] Obtained from fitting to the Berry first order polynomial. Results are mean±std of duplicate determinations

Table 2. Solution characteristics of different aqueous concentrations of *Bauhinia monandra* galactomannan under steady shear and small deformation oscillations at 25°C.

	a. Parameters of the Williamson model fitted to viscosity-shear rate curves				b. Frequency sweep data showing G crossover point at critical angular frequency		
Conc (wt%)	η_o(Pa.s)	τ (s)	N	s.e.	G (Pa)	ω_{crit} (rad/s)	$\tau'=(1/\omega_{crit})$ (s)
0.50	0.248	0.04314	0.5117	14.24			
0.75	1.583	0.1932	0.5943	15.47	17.19	64.10	0.0156
1.0	7.179	0.7159	0.6212	20.69	31.47	38.26	0.0261
1.5	63.55	2.521	0.7021	17.18	57.29	8.619	0.1160
2.0	244.2	5.556	0.7383	15.99	90.66	3.309	0.3022

Key: η_o (Pa.s)= Zero shear viscosity, τ (s) = Williamson relaxation time, N = Williamson rate index, s.e.= Standard error. G = modulus at crossover point (Pa), ω_{crit} = critical angular frequency (rad/s), τ'=time for microstructural coupling

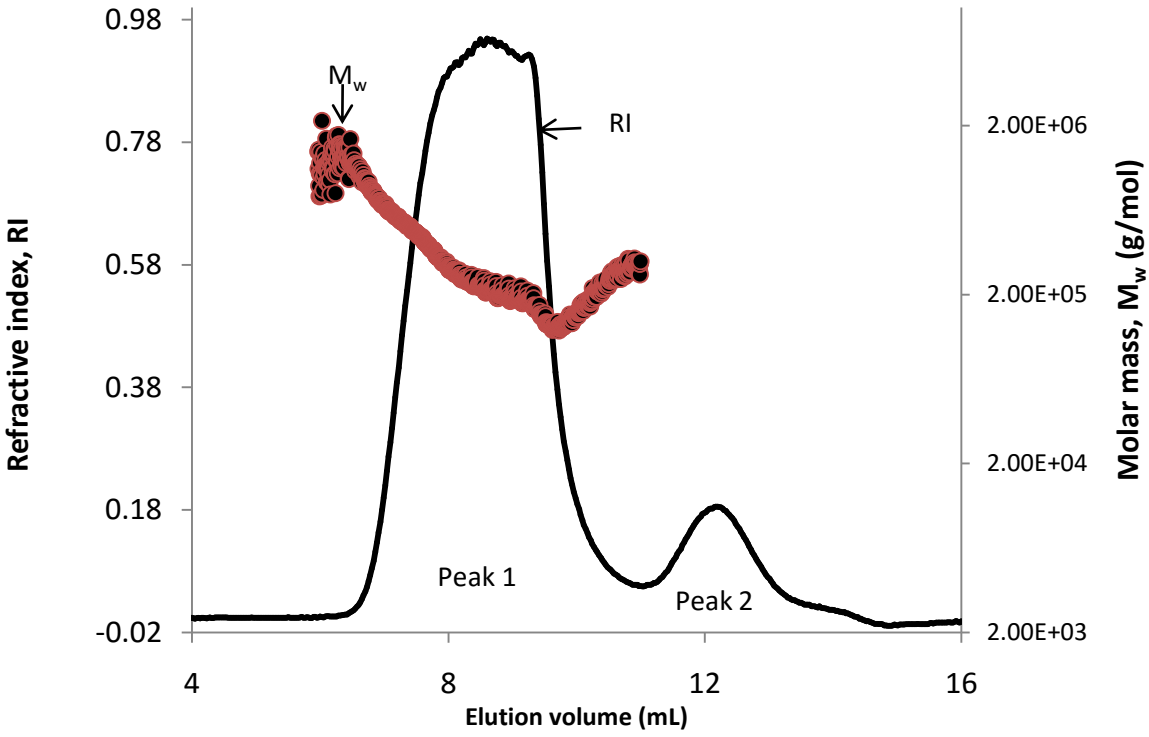

Figure 1. GPC-MALLS showing M_w and RI response peaks versus elution volume of *B. monandra* galactomannan.

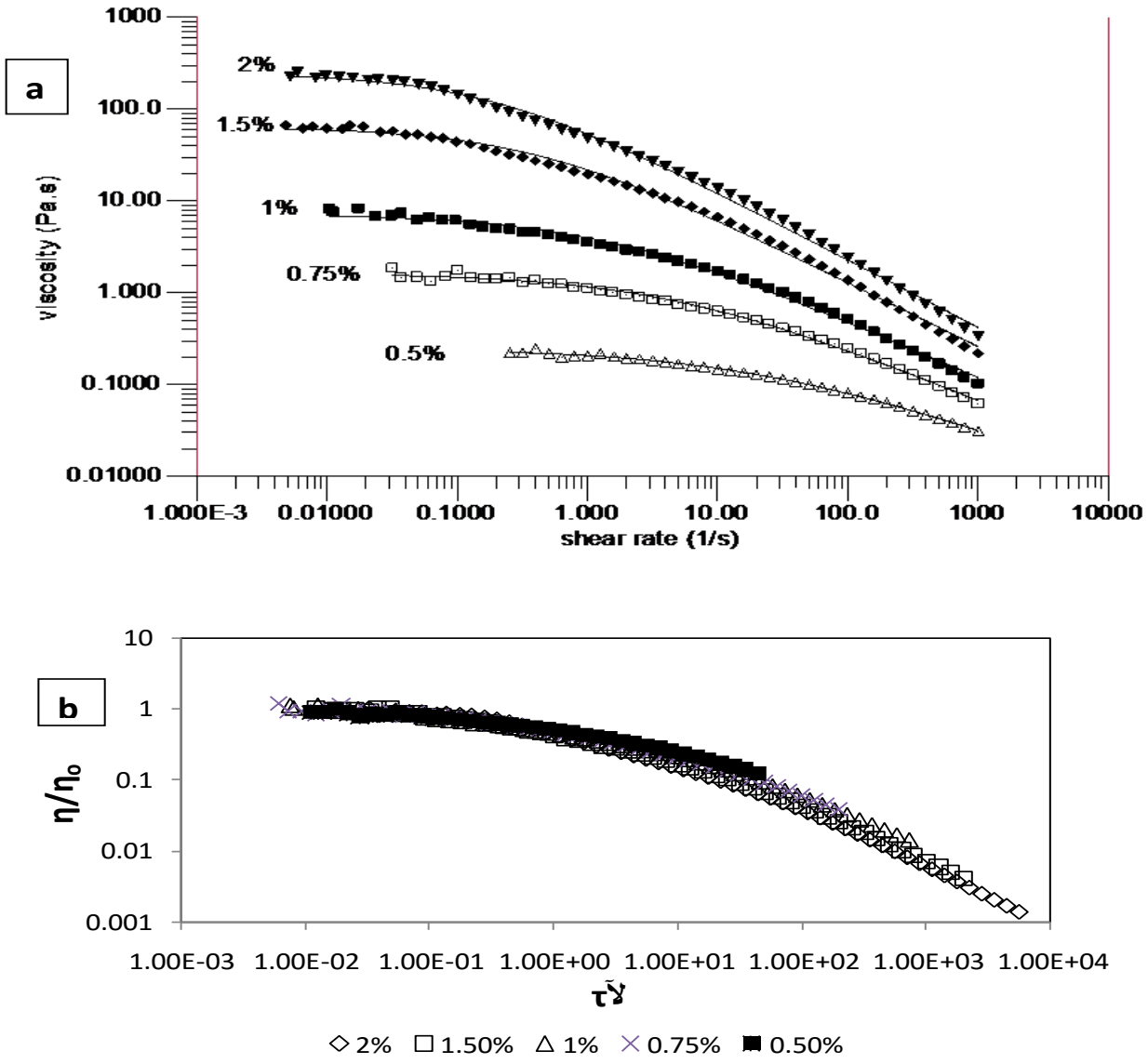

Figure 2 (a). Viscosity - shear rate profiles for different concentrations of *B. monandra* galactomannan at 25^{o}C fitted to the Williamson model. (b). Plots of reduced viscosity versus time constant for varying concentrations of *B. monandra* galactomannan

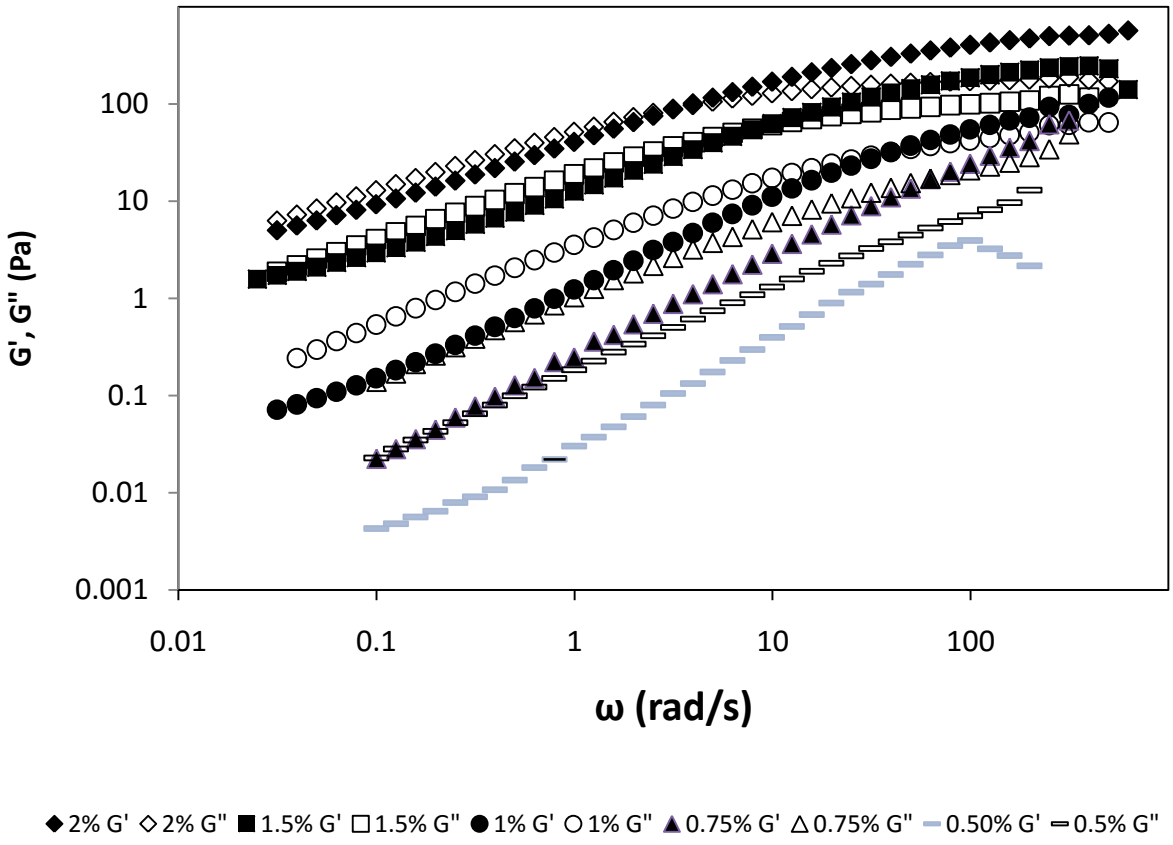

Figure 3. Frequency sweep showing G′ and G″ (storage and loss moduli) versus ω (angular frequency) for different polymer concentrations at 25^{o}C

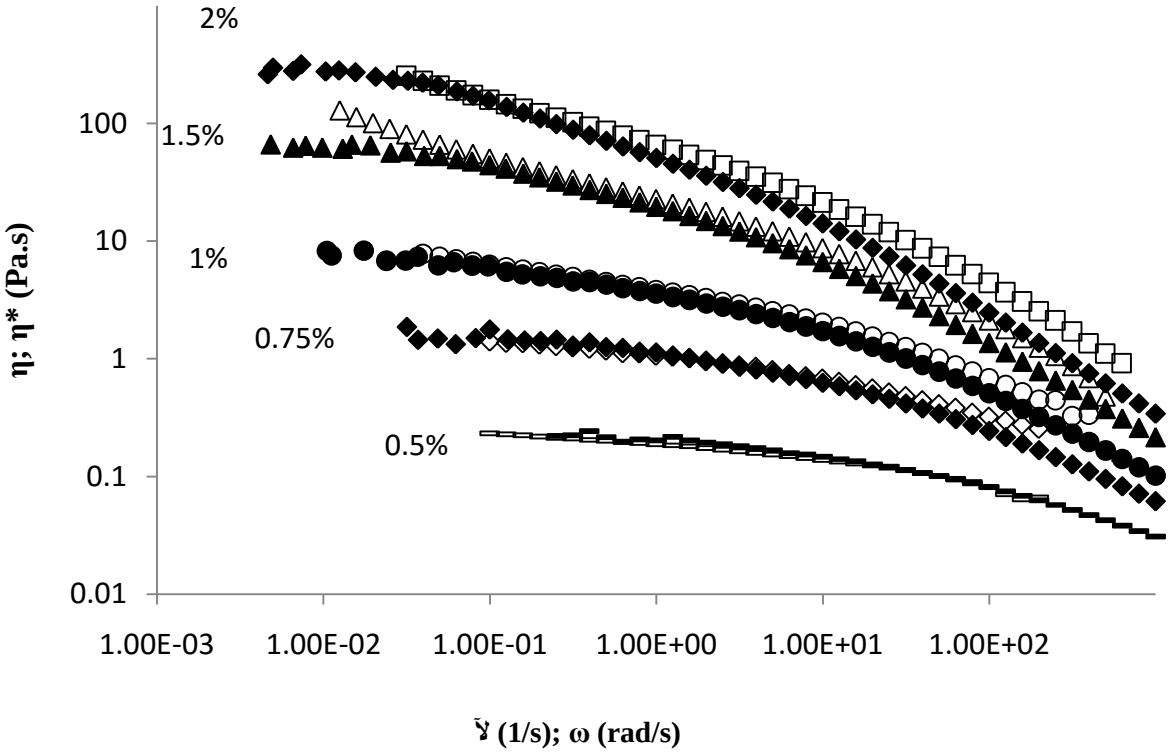

Figure 4. Cox-Merz plot: Superimposition of steady shear viscosity (η(γ̇)) [filled symbols] and dynamic viscosity (η*(ω)) [unfilled symbols]measured at 25^{o}C for different concentrations of *B. monandra* galactomannan

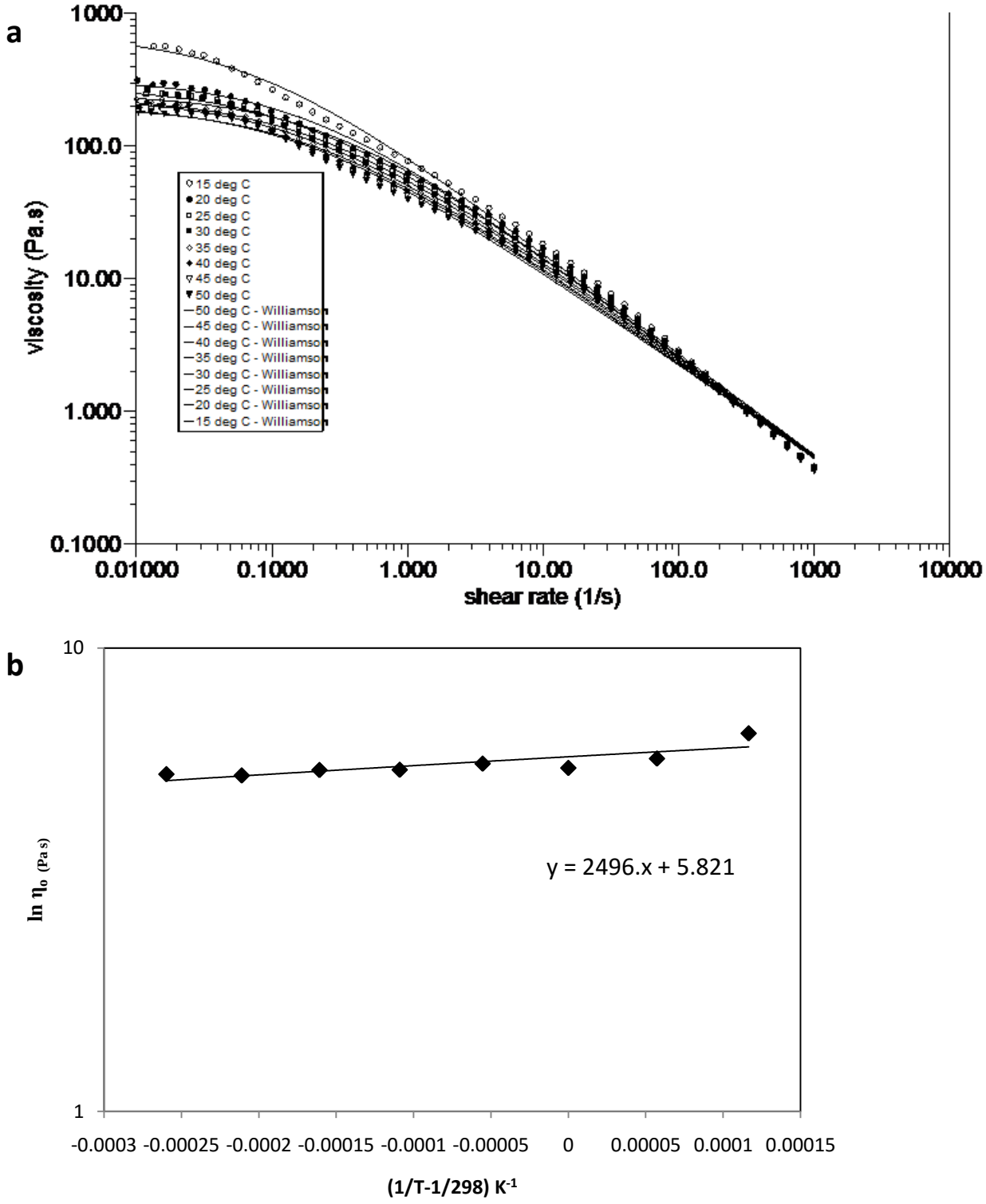

Figure 5 a. Viscosity-shear rate profiles of 2% *B. monandra*galactomannan at different temperatures.b). Arrhenius plot of zero shear viscosity as a function of inverse absolute temperature

Supplementary file

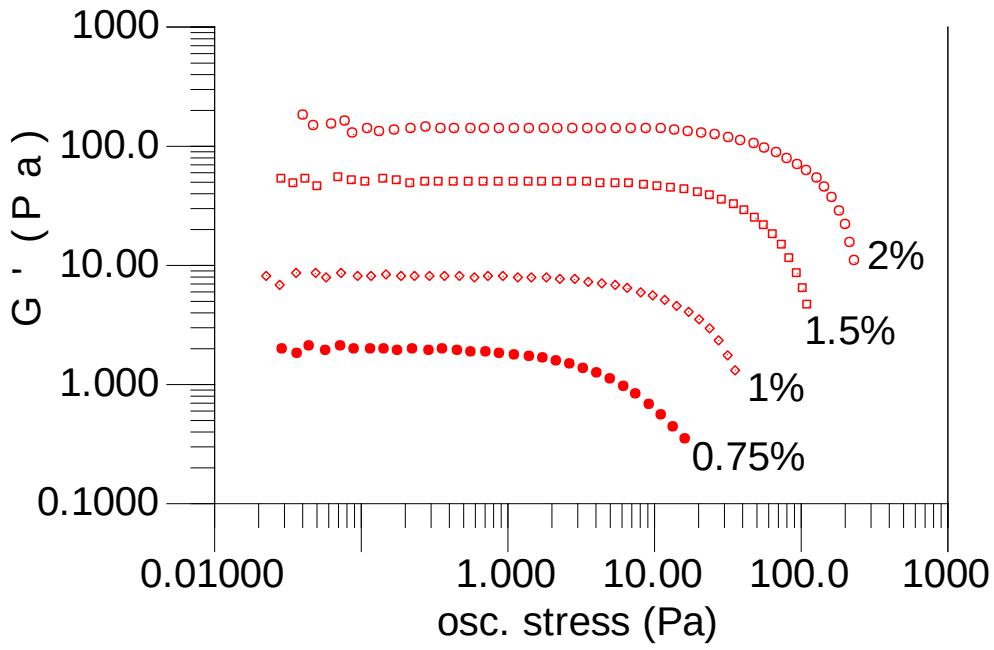

Figure S1. Oscillation stress sweep showing storage modulus, G′ at different polymer concentrations at 25°C